Supplemental Data

1 Radiotracer Synthesis

Carrier-free ^{18}Fluoride was produced via the $^{18}O(p,n)^{18}F$ nuclear reaction at a Cyclone 18/9 cyclotron (IBA, Louvain-la-Neuve, Belgium) by irradiation of enriched ^{18}O-water. ^{18}Fluoride was immobilized on an anion-exchange cartridge (QMA Light; Waters; preconditioned with 0.5M K_2CO_3-solution (5mL) and H_2O (5-10mL)). The cartridge was washed two times with water for injection (2mL) and eluted with 0.9% NaCl-solution (1.5mL) through a sterile filter into a sterile, pyrogen-free vial. The solution of ^{18}Fluoride was directly used for biological applications without further formulation. The mean activity obtained for the experiments was 4.15GBq.

The synthesis of ^{18}F-FMISO was carried out according to the procedure described by Kämäräinen et al. (*1*). After an overall synthesis time of 80min the decay-corrected radiochemical yield was 40% on an average with a maximum activity amount of 14GBq isolated product ^{18}F-FMISO. The radiochemical purity was $\geq$95% and the specific activity (end of synthesis) was always $\geq$50GBq/µmol. ^{18}F-FMISO was identified by co-injection with its non-radioactive reference compound by analytical HPLC. ^{18}F-Fluorothymidine (^{18}F-FLT) was synthesized as described by Kim et al. (2) with radiochemical purity > 99% and specific activity > 50GBq/µmol. ^{18}F-FDG, ^{18}F-Fluorocholine (^{18}F-FCH) and ^{18}F-Fluoroethyltyrosine (18F-FET) were obtained from routine productions for clinical use at the University Hospital Zurich.

2 Quantitative analysis of ^{18}F-FDG uptake in the LM8 model

2.1 Experimental procedure

In mice with LM8 cell-derived tumors, ^{18}F-FDG was injected in a final volume of 100µl into a lateral tail vein in awake mice (9.5-16.4MBq).

Muscle uptake of ^{18}F-FDG was higher in the control than in the tumor bearing leg. Consequently, for the calculation of the ratio between tumor and a reference area the hip was used as the control VOI in this model. For these mice, VOIs were drawn with the use of the CT images (Supplemental Fig. 1).

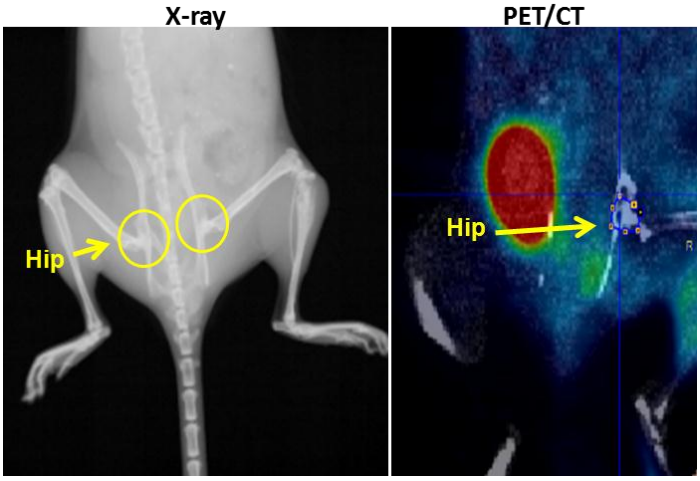

Supplemental Figure 1: Representative delineation of the hip area used as healthy control tissue for ^{18}F-FDG uptake in non-anesthetized mice with LM8 cell line-derived intratibial osteosarcoma. X-ray image (left) shows the hip area (within yellow circles) that defined the region of interest in the corresponding combined PET/CT image (right).

3 Quantitative data from immunohistology

3.1 Experimental procedure

The staining protocol is the same as described in the Materials and Methods of the paper. However specifically for the quantitative analysis of Ki67 positivity we used Alexa Fluor 546-labeled secondary antibodies. Since Ki67 protein localizes in the nuclei, DAPI was used for counterstaining. Fluorescent and DAPI images were taken with a Nikon Microscope ECLIPSE E600 equipped with appropriate filter blocks and Image J program was then used to count all the nuclei (staining with DAPI) and the ones positive for Ki67 in order to calculate the percentage of Ki67-stained cells. We stained three slides for each mouse model with a minimum of 100μm difference in the depth from each other and we took six to eight pictures for each slide.

Due to the location of CaIX in the cell membrane, we could not use immunofluorescence in order to perform a quantitative analysis as we did for Ki67. We therefore applied the staining protocol described in the paper and the analysis was done using a custom made MATLAB (v2009b, Mathworks Inc., Natick, MA, USA) program. Through a deconvolution theory the brown (CaIX) staining and the blue (hematoxylin) counterstaining were separated and the percentage of the brown stained area compared to the total tissue area was calculated (3). Much like for the analysis of Ki67 staining, we stained three randomly selected tissue sections that were collected >100μm apart from individual tumors of each mouse model. On individual 6μm thick sections we randomly selected six to eight images for the analysis.

The graphs and the statistics were obtained with GraphPad Prism® 5.01 Network software.

3.2 Results

The linear regression analysis data show a significant ($p<0.0005$) correlation between Ki67 staining and tumor uptake of ^{18}F-FDG (Supplemental Fig. 2A) and a significant difference ($p<0.001$) between the percentage of Ki67 stained cells in the 143B model compared to the SaOS-2/Caprin-1 model, which relates to the difference observed in the quantitative analysis of ^{18}F-FDG tumor uptake (Supplemental Fig. 2B). In the LM8 model tumors only two mice were available for analysis. Nevertheless the data show the tendency for a lower percentage of Ki67 stained cells in the SaOS-2/Caprin-1 compared to the other two models. This finding is consistent with the results obtained with the PET imaging where animals with SaOS-2/Caprin-1 cell derived tumors showed the lowest ratio of ^{18}F-FDG uptake between the tumor and the control leg.

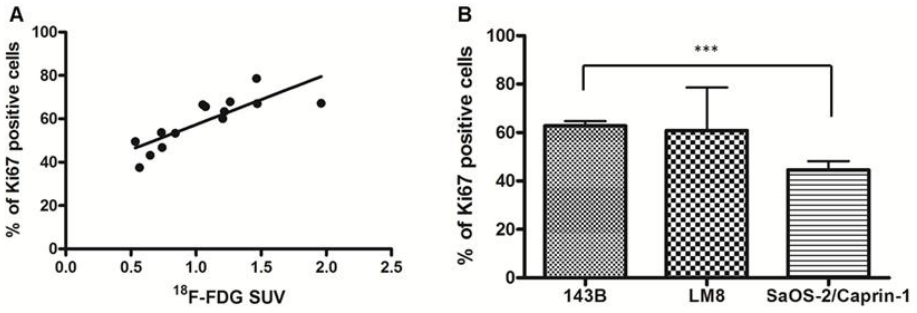

Supplemental Figure 2: Linear regression analysis of Ki67 immunostaining in tumor tissue sections and ^{18}F-FDG tumor uptake (R^2=0.67; n=14; p<0.005) (A) and comparison of the percentage of Ki67 stained cells in the three different osteosarcoma mouse models (p<0.005) (B).

Regarding the quantitative analysis of CaIX, we could observe a significant (p<0.05) correlation between the percentage of CaIX stained cells and the tumor uptake of ^{18}F-FMISO (Supplemental Fig. 3A) and a comparison of the percentage of CaIX stained cells in the individual mouse models (Supplemental Fig. 3B) are shown below. The 143B and SaOS-2/Caprin-1 models show a significantly higher percentage of CaIX stained cells than the LM8 model (p<0.05), which is in good agreement with the ^{18}F-FMISO tumor uptake.

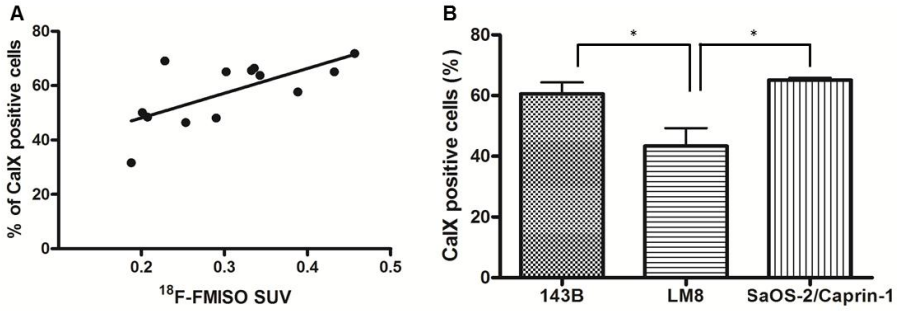

Supplemental Figure 3: Linear regression analysis of CaIX immunostaining in tumor tissue sections and ^{18}F-FMISO tumor uptake (R^2=0.46; n=13; p<0.05) (A) and comparison of the percentage of CaIX stained cells in the three osteosarcoma models (p<0.05) (B).

4 Tumor Monitoring in the Three Osteosarcoma Models by X-ray

4.1 Experimental procedure

The development of primary tumors was monitored by X-ray (Faxitron, Arizona, USA) weekly for 143B and LM8 cell-derived tumors and once every two weeks for the slowly developing SaOS-2/Caprin-1 cell derived tumors.

4.2 Results

The three osteosarcoma mouse models were chosen based on their well-defined radiological phenotypes (*4*). 143B tumor bearing mice developed characteristic osteolytic lesions that became detectable by X-ray analysis two weeks after tumor cell injection (Supplemental Fig. 4). The LM8 cell derived tumors showed a mild osteoblastic phenotype on X-ray with soft tissue swelling 2 weeks after cell injection. SaOS-2/Caprin-1 cell derived tumors showed a more pronounced osteoblastic phenotype with similar osteoblastic clouds in all mice despite considerable heterogeneity in the timing of tumor development in individual animals.

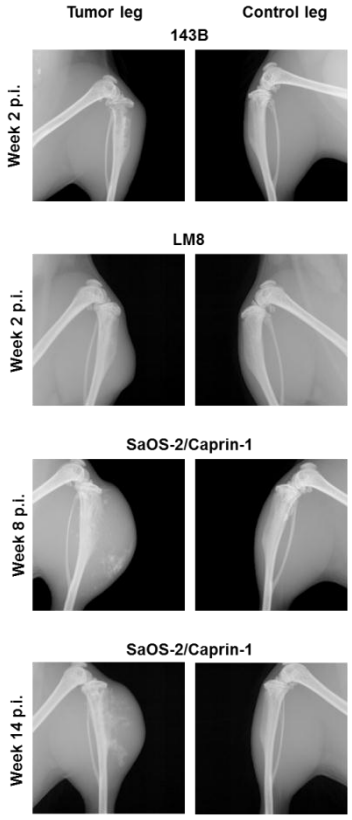

Supplemental Figure 4: X-ray of representative intratibial primary tumors and of the corresponding control leg in indicated mouse models. p.i. = post tumor cell injection.

5 Uptake of ^{18}F-Fluorothymidine (^{18}F-FLT), ^{18}F-Fluorocholine (^{18}F-FCH) and ^{18}F-Fluoroethyltyrosine (^{18}F-FET) in osteosarcoma mouse models

5.1 Experimental procedure

The animal model and the PET protocol used for this pilot study was the same used for ^{18}F-FDG, ^{18}F-FMISO and ^{18}Fluoride described in the Materials and Methods.

5.2 Results

A pilot study on the uptake of these tracers in osteosarcoma mouse models has been performed. We investigated ^{18}F-FCH and ^{18}F-FET in the 143B model and ^{18}F-FLT in the 143B and LM8 models.

These tracers were not taken up reproducibly by tumor tissue in individual mice of the same model. Supplemental Figure 5 and 6 show representative PET images obtained with ^{18}F-FCH, ^{18}F-FET and ^{18}F-FLT. Only two out of four tumors in 143B mice showed a detectable uptake of ^{18}F-FET and ^{18}F-FCH (Supplemental Fig. 5A, C), while there was no difference between lesion and control leg in the other two mice (Supplemental Fig. 5B, D).

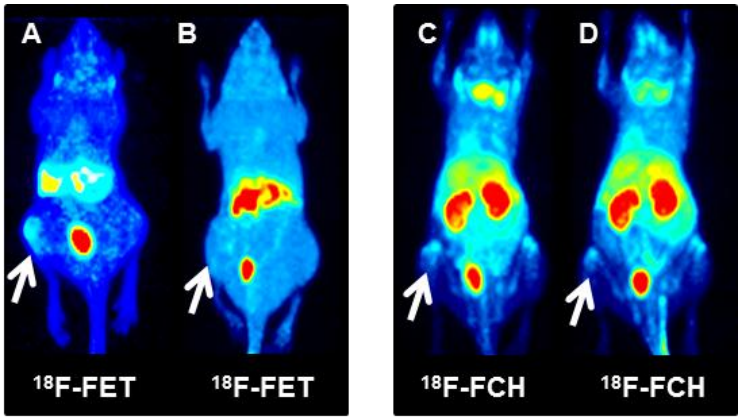

Supplemental Figure 5: Representative PET images of 143B tumor bearing mice that received ^{18}F-FET (A, B) and ^{18}F-FCH (C, D). Arrows point to the locations of the tumor.

^{18}F-FLT uptake was not detectable in the 143B model (Supplemental Fig. 6); in the LM8 model, tracer uptake was visible but at a low level. Based on these results, we decided to exclude ^{18}F-FET, ^{18}F-FCH and ^{18}F-FLT from further experiments and to focus on ^{18}F-FDG, ^{18}F-FMISO and ^{18}Fluoride that gave more reproducible results in a pilot study with the 143B and LM8 models.

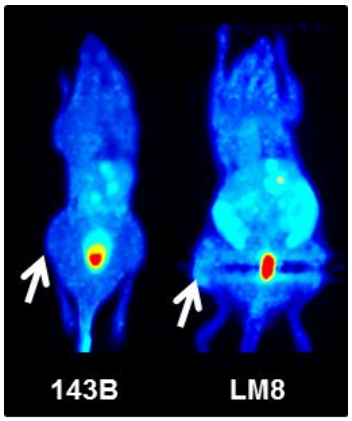

Supplemental Figure 6: Representative PET images of mice that received ^{18}F-FLT in the indicated animal models

Supplemental references

1. Kämäräinen EL, Kyllönen T, Nihtilä O, et al. Preparation of fluorine-18-labelled fluoromisonidazole using two different synthesis methods. *J Label Compd Radiopharm*. 2004;47:37-45.

2. KimWD, Ahn D, Oh Y, et al. New class of SN2 reactions catalyzed by protic solvents: facile fluorination for isotopic labeling of diagnostic molecules. *J Am Chem Soc*. 2006;128:16394–16397.

3. Ruifrok AC, Johnston DA. Quantification of histochemical staining by color deconvolution. *Anal Quant Cytol Histol*. 2001;23:291-299.

4. Yuan J, Ossendorf C, Szatkowski JP, et al. Osteoblastic and osteolytic human osteosarcomas can be studied with a new xenograft mouse model producing spontaneous metastases. *Cancer Invest*. 2009;27:435-442.